OPEN

Correspondence and
requests for materials
should be addressed to
B.W. (wenbin@ysu.
edu.cn)

Relative importance of grain boundaries and size effects in thermal conductivity of nanocrystalline materials

Huicong Dong[1], Bin Wen[1] & Roderick Melnik[2]

[1]State Key Laboratory of Metastable Materials Science and Technology, Yanshan University, Qinhuangdao 066004, China,
[2]M²NeT Lab, Wilfrid Laurier University, Waterloo, 75 University Ave. West, Ontario, Canada N2L 3C5.

A theoretical model for describing effective thermal conductivity (ETC) of nanocrystalline materials has been proposed, so that the ETC can be easily obtained from its grain size, single crystal thermal conductivity, single crystal phonon mean free path (PMFP), and the Kaptiza thermal resistance. In addition, the relative importance between grain boundaries (GBs) and size effects on the ETC of nanocrystalline diamond at 300 K has been studied. It has been demonstrated that with increasing grain size, both GBs and size effects become weaker, while size effects become stronger on thermal conductivity than GBs effects.

As a critically important physical property, thermal conductivity of nanocrystalline materials is of quite general interest due to its significant technological importance in many practical applications of such materials, including bioMEMs[1], thermal barrier coatings[2] and micro-/nanoelectromechanical devices[3], to name just a few. It is well known that nanocrystalline materials are structurally characterized by a large volume fraction of grain boundaries (GBs)[4]. Generally, GBs can be considered as an obstacle for heat transmission. Therefore, thermal conductivity of nanocrystalline materials is lower than that of the corresponding single crystal materials, and it decreases with decreasing grain sizes[5].

Many efforts have been devoted to the research on nanocrystalline materials thermal conductivity[2,5–7], and some equations to model effective thermal conductivity (ETC) have been developed. In 1998, a Kapitza resistance-EMA (effective medium approaches) model to describe the ETC for common polycrystals with isotropic, equisized spherical crystallites has been proposed by Nan and Birringer[5], where the ETC can be described as

$$K = \frac{K_0}{1 + 2R_K K_0/d}. \tag{1}$$

In (1), K_0 is single crystal thermal conductivity ($W/m \cdot K$), R_K is Kapitza thermal resistance from GBs ($m^2 K W^{-1}$), and d is grain size (nm).

By considering that each grain boundary region is shared by two grains, Eq. (1) has been revised by Yang et al. in 2002[2], which led to the following expression:

$$K = \frac{K_0}{1 + R_K K_0/d}. \tag{2}$$

It is different from Eq. (1) only by the absence of a coefficient factor 2 for R_K.

Although Eq. (2) has been widely used to study the ETC for many nanocrystalline materials[2,3,8–13], in fact, its value calculated by Eq. (2) is usually larger than almost all of the experimental or simulated values[3,9,12]. A persuasive explanation for this inconformity is that an intragranular thermal transmission property may change with grain size[12]. It is collectively known as size effects of thermal properties. The reason for these effects is that the phonon mean free path (PMFP) is reduced due to increased phonon scattering in the intragranular with decreasing grain size. By considering size effects of thermal properties[14–17], a new type ETC formula[15,16] for nanocrystalline materials has been suggested as

$$K = \frac{K_{intra}}{1 + R_K K_{intra}/d}, \tag{3}$$

where K_{intra} is the intragranular thermal conductivity ($W/m \cdot K$), and R_K is the Kapitza thermal resistance (intergranular thermal resistance). In this theoretical model, the ETC for nanocrystalline materials is not only

affected by the Kapitza thermal resistance, but also by size effects. As a result, an agreement between calculated and experimental results has been reached[15].

Although Eq. (3) has been proved to be reasonable for calculating the ETC of nanocrystalline materials, it is not a convenient model for applications, especially in the process of computing intragranular thermal conductivity. To make Eq. (3) better amenable to practical application, a simple theoretical ECT model for nanocrystalline materials has been proposed in this work by considering both single crystal thermal properties and the Kaptiza thermal resistance. By comparing our theoretical predictions with simulated results for the ECT of nanocrystalline diamond at 300 K as well as experimental ETC of nanocrystalline silicon[14,15,18] at 300 K, a good agreement between them has been obtained, which proves the rationality behind our ECT formula. Although the effect of both GBs and size effects can be expressed by using the grain size in this ECT formula, the mechanisms of action in these two factors on ETC are totally different[15,19,20], and further the contribution of these two factors on ETC may be different for different materials and grain sizes. Therefore, it is necessary to study the effect of each factor on ETC separately. In this work, the relative importance of GBs and size effects has also been studied by using our suggested theoretical model. In what follows, we explain this in detail.

For Eq. (3), the greatest challenge in quantitatively predicting the ETC for nanocrystalline materials is to calculate intragranular thermal conductivity K_{intra}. To calculate the intragranular thermal conductivity, kinetic theory[14] has been used, leading to the following expression:

$$K_{intra} = \frac{1}{3} C v \Lambda_{intra}, \qquad (4)$$

Λ_{intra} is the intragranular PMFP due to size effect of thermal properties, and the value of Λ_{intra} is correlated with single crystal PMFP Λ_0, as well as with an additional PMFP Λ_{add} due to decreased grain sizes.

By using Matthiessen's rule[14], their relationship can be written as

$$\Lambda_{intra}^{-1} = \Lambda_0^{-1} + \Lambda_{add}^{-1}. \qquad (5)$$

As a result, intragranular PMFP Λ_{intra} can be expressed as

$$\Lambda_{intra} = \frac{\Lambda_0 \Lambda_{add}}{\Lambda_0 + \Lambda_{add}}. \qquad (6)$$

Assuming that the acoustic velocity and heat capacity are not affected by grain size, when Eq. (6) is inserted into Eq. (4), the intragranular thermal conductivity can be described as

$$K_{intra} = \frac{1}{3} C v \Lambda_0 \frac{\Lambda_{add}}{\Lambda_0 + \Lambda_{add}} = \frac{K_0}{1 + \Lambda_0/\Lambda_{add}}, \qquad (7)$$

where K_0 is the corresponding single crystal thermal conductivity ($W/m \cdot K$).

Hence, the intragranular thermal conductivity K_{intra} can be considered as a function of the corresponding single crystal thermal conductivity K_0 and PMFP Λ_0, as well as grain size induced PMFP Λ_{add}. It is well known that Λ_{add} is related to grain size d. For a definitive material under a given temperature, single crystal thermal conductivity K_0 and PMFP Λ_0 can be regarded as constants. Therefore, the intragranular grain thermal conductivity can be described as a function of grain size d. According to Ref. 21, the thermal conductivity of nanocrystalline materials can be modeled by an exponential function of defect concentration. In this work, we assume that the grain boundary is a type of defect, and that the intragranular grain thermal conductivity can be expressed as an exponential function of grain size d. Therefore, we have

$$K_{intra} = \frac{K_0}{1 + \Lambda_0/d^\alpha}, \qquad (8)$$

where α is the exponent ranging from 1/2 to 3/4 according to phenomenological theory[22].

Now, by combining the equations (3) and (8), the ETC of nanocrystalline materials can be written as

$$K = \frac{K_0/(1 + \Lambda_0/d^\alpha)}{1 + R_K [K_0/(1 + \Lambda_0/d^\alpha)]/d}. \qquad (9)$$

To determine an affirmatory value of α, a simulated ETC of nanocrystalline silicon[17] at 500 K is used to fit Eq. (9) by using the least square method[23]. At the same time, in this calculation we use the single crystal silicon thermal conductivity K_0 at 500 K from experimental data ($77 W/m \cdot K$)[24], R_K value ($1.06 \times 10^{-9} \ m^2 KW^{-1}$) and Λ_0 (17.6 nm) from simulation[17]. As a result, the determined value of α is 0.75 with a correlation coefficient about 0.93, which shows that the value of α agrees with the phenomenological theory[22].

Finally, the ETC of nanocrystalline materials can be described as

$$K = \frac{K_0/(1 + \Lambda_0/d^{0.75})}{1 + R_K [K_0/(1 + \Lambda_0/d^{0.75})]/d}. \qquad (10)$$

By using this equation, the ETC of nanocrystalline materials can be easily obtained based only on its grain size d, single crystal thermal conductivity K_0, single crystal PMFP Λ_0, and the Kaptiza thermal resistance R_K.

To further validate this equation, our present theoretically predicted ETC of nanocrystalline diamond has been compared with molecular dynamic (MD) simulated results. The MD calculated ETC of nanocrystalline diamond at room temperature is shown in Fig. 1 with a grain size range from 2 to 13.3 nm. By comparing our simulated results with previously reported ETC values for nanocrystalline diamond[9], we confirm that a good agreement has been obtained. This has also confirmed that the MD simulation parameters used in this work are reliable.

In order to get theoretical values of ETC for nanocrystalline diamond from Eq. (10), the single crystal diamond thermal conductivity and the Kaptiza resistance of crystalline diamond grain boundary have also been calculated by using MD simulation, and details for these calculations can be found in supplementary document (Supplementary discussions 2 and 3). The calculated values of K_0 and R_K are 1265 $Wm^{-1}K^{-1}$ and 0.143 $\times 10^{-9}$ m^2KW^{-1}, respectively. Both calculated values of K_0 and R_K are consistent with the previously reported results[9,20,25,26], confirming that our computational method is reliable. The value of single crystal PMFP Λ_0 used in the calculation has been chosen as 180 nm, which is in the range of previously reported values (150 nm[20] and 400 nm[27]). By comparing ETCs of nanocrystalline diamond obtained from MD simulations with theoretical analysis based on our model (as plotted in Fig. 1), a good agreement between them has been observed, demonstrating that
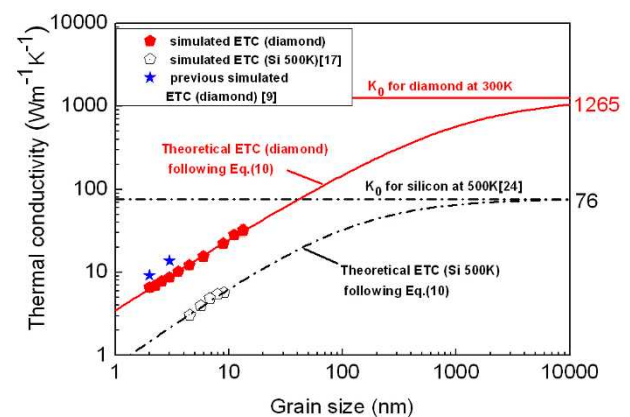

Figure 1 | Grain-size dependence of thermal conductivity for nanocrystalline diamond (300 K) and silicon (500 K).

our newly developed model for ETC is effective for nanocrystalline materials. In addition, a good agreement between our model and experimental ETC[14,15,18] for nanocrystalline silicon at 300 K (refer to Supplementary discussion 4 and Fig. S7) has also been observed, which further confirmed that our model is valid.

Since both, the effect of GBs and size effects of thermal properties, are considered in our calculations, the ETC of nanocrystalline diamond is much smaller than the single crystal diamond thermal conductivity, and it decreases with the reduced grain sizes. The reduction of thermal conductivity in nanocrystalline diamond compared with single crystal is caused by two factors: GBs and size effects of thermal properties. The relative importance of these two groups of effects on the reduced thermal conductivity of nanocrystalline materials is a very important issue for the study of nanocrystalline materials thermal conductivity. In this work, the relative importance of these two effects on the reduced thermal conductivity of nanocrystalline materials has been studied by using nanocrystalline diamond as a prototype. Note that the thermal resistance of nanocrystalline diamond R_{pol} can be divided into two parts, one is the intragranular thermal resistance (R_{intra}) caused by size effects, and the other one is the intergranular thermal resistance (R_K/d) caused by GBs. The plots of intragranular thermal resistance (R_{intra}), intergranular thermal resistance (R_K/d), and total thermal resistance (R_{pol}) of nanocrystalline diamond have been obtained as functions of grain size, based on Eq. (10). They can be seen in Fig. 2 (a). Note that theoretical results from our theoretical model agree well with the results obtained by MD simulations. With the increasing grain size, the intragranular thermal resistance R_{intra} and intergranular thermal resistance R_K/d both decrease. When the grain size is large enough (or $1/d$ tends to 0), the intragranular thermal resistance approaches to the single crystal thermal resistance, while the intergranular thermal resistance tends to zero. These results demonstrate that with increasing grain size, both the effect of GBs and the size effects become weaker.

To better understand the relative importance of GBs and size effects of thermal properties on the reduced thermal conductivity of nanocrystalline diamond, the ratio of intragranular thermal resistance, as well as the intergranular thermal resistance, to the total nanocryatlline diamond thermal resistance (R_{intra}/R_{pol} and (R_K/d)/R_{pol}) have been calculated. These characteristics have been plotted in Fig. 2 (b). As can be seen from Fig. 2 (b), R_{intra}/R_{pol} is larger than (R_K/d)/R_{pol} throughout, and with increasing grain size, the value of R_{intra}/R_{pol} is increasing, while the value of (R_K/d)/R_{pol} is decreasing. It indicates that with increasing grain size, size effects of thermal properties become stronger than the GBs effect on nanocrystalline diamond thermal conductivity at 300 K. When the grain size is less than 10 nm, R_{intra}/R_{pol} is less than 0.65, and (R_K/d)/R_{pol} is larger than 0.35, the effect of GBs and size effects of thermal properties both play a very important role for ETC. When the grain size is 100 nm, R_{intra}/R_{pol} is 0.79, and (R_K/d)/R_{pol} is 0.21, size effects of thermal properties become much stronger than the effect of GBs on ETC, and both effects are still very important. When grain size is 1000 nm, R_{intra}/R_{pol} is 0.92, and (R_K/d)/R_{pol} is 0.08, size effects of thermal properties are still relatively stronger than the effect of GBs on ETC. When the grain size is 10000 nm, R_{intra}/R_{pol} is 0.99, and (R_K/d)/R_{pol} is only 0.01, at that time, both effects have almost no influence on ETC, and the nanocrystalline diamond thermal conductivity becomes very close to the corresponding single crystal thermal conductivity. Analysis of relative importance of size effects and GBs on ETC shows that besides GBs, size effects also play a very important role in the reduced ETC, which is a good reason for the inconformity between previous theoretical results and simulated or experimental ones[3,9,12], and that can be explained by decreasing intragranular PMFP and increasing GB number due to decreasing grain size.

In addition, the thermal transmission of nanocrystalline silicon at 500 K[17] have also been studied on the basis of Eq. (10). As shown in Fig. 1 and Fig. 2 (a), the simulated values of thermal conductivity and
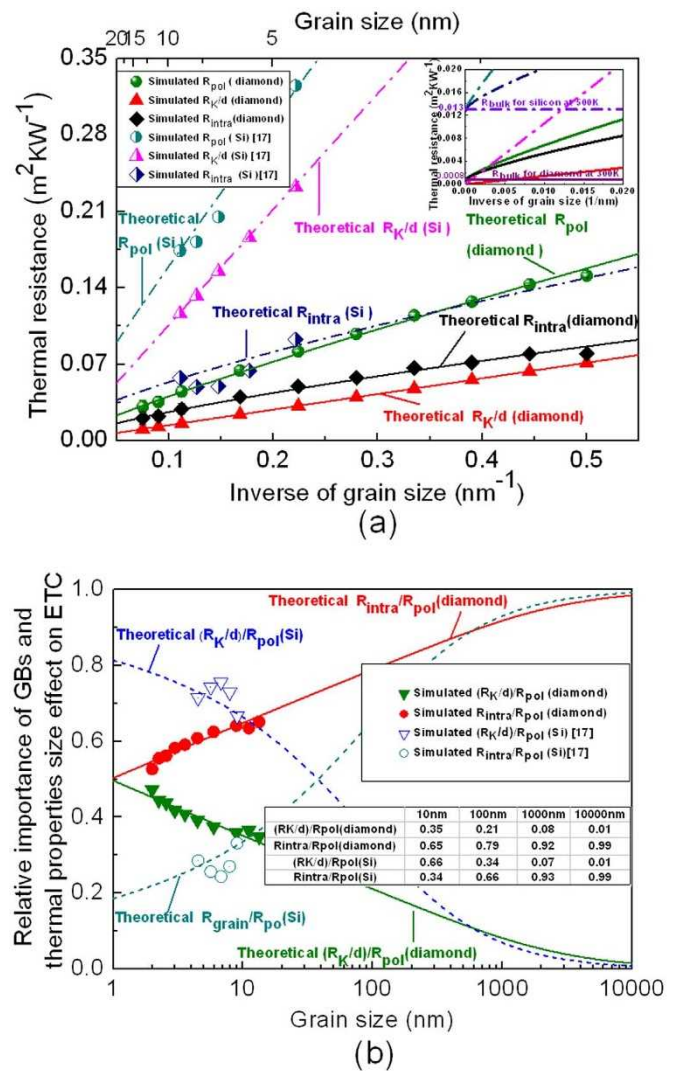

Figure 2 | Relative importance of GBs and size effects of thermal properties on ETC of nanocrystalline diamond (300 K) and silicon (500 K). (a). Grain-size dependence of thermal resistance for nanocrystalline diamond (300 K) and silicon (500 K). Inset: magnified grain-size dependence of thermal resistance for nanocrystalline diamond (300 K) and silicon (500 K), when $1/d$ tends to 0, $R_{pol} = R_{intra} = R_0$, $R_K/d = 0$. (b) Relative importance of GBs and size effects of thermal properties on ETC in nanocrystalline diamond (300 K) and silicon (500 K).

thermal resistance of nanocrystalline silicon[17] at 500 K conform well with our theoretical model. With increasing grain size, both the effect of GBs and size effects of thermal properties on ETC both become weaker. However, the relative importance of GBs and size effects of thermal properties on ETC for nanocrystalline silicon at 500 K is different from that of nanocrystalline diamond at 300 K. For nanocrystalline silicon at 500 K, the effect of GBs is stronger than size effects on ETC when $d < 40$ nm, whereas a crossover is observed at $d = 40$ nm, while for $d > 40$ nm, the size effects of thermal properties are stronger. This difference indicates that besides grain size, perhaps material kind and temperature are also important factors that affect the relative importance of GBs and size effects of thermal properties on ETC. Moreover, the relative importance of GBs and size effects for nanocrystalline silicon at 300 K has also been analyzed by applying our theoretical model. Although the trend is the same as that of nanocrystalline silicon at 500 K and nanocrystalline diamond at 300 K, the critical grain size is different for different materials and temperature (Detail in Supplementary discussion 5).
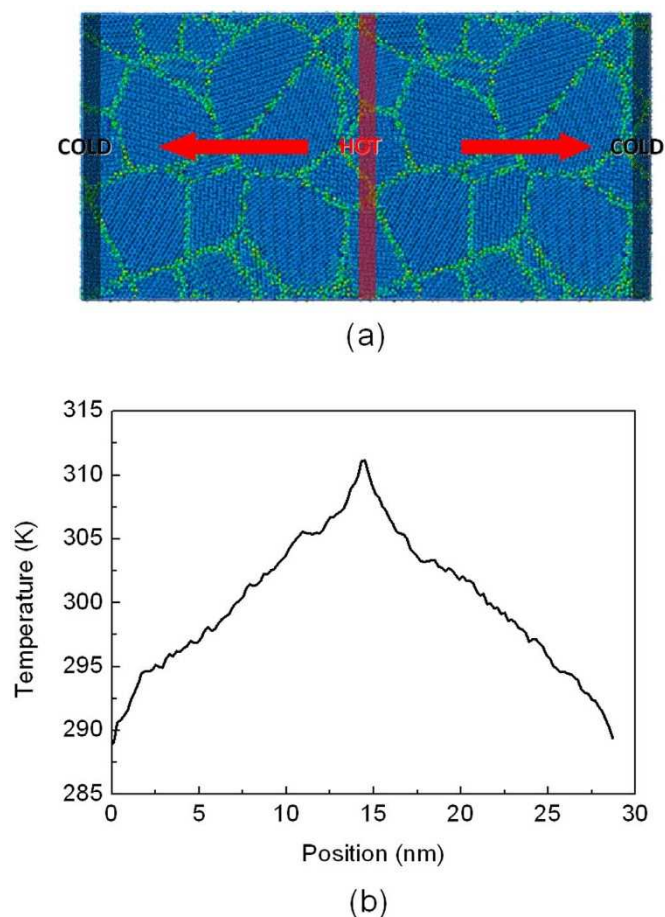
(a)

(b)

Figure 3 | Schematic diagram of NEMD approach for calculating nanocrystalline diamond thermal conductivity. (a) Atomic structure model of nanocrystalline diamond, the cold regions are placed at the ends of the sample, while the hot region is located in the middle. (b) Temperature profile along the heat flow direction.

In summary, a theoretical model for describing the ETC has been proposed in this work. By using this theoretical model, the ETC for nanocrystalline materials can be easily obtained by using only its
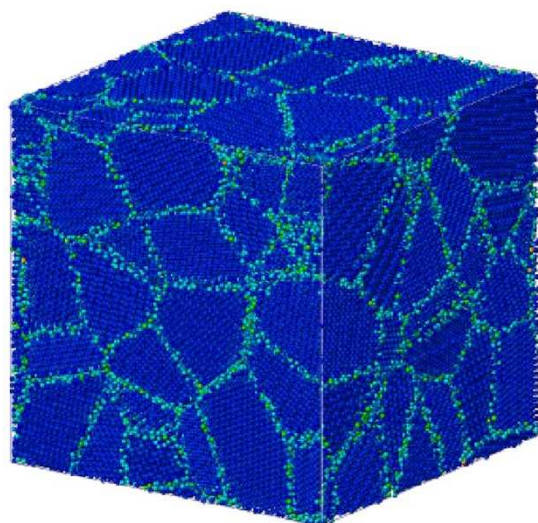
Figure 4 | Typical nanocrystalline diamond models created by the three-dimensional Voronoi tessellation method, the intragranular atoms are blue, and the grain boundary atoms are green.
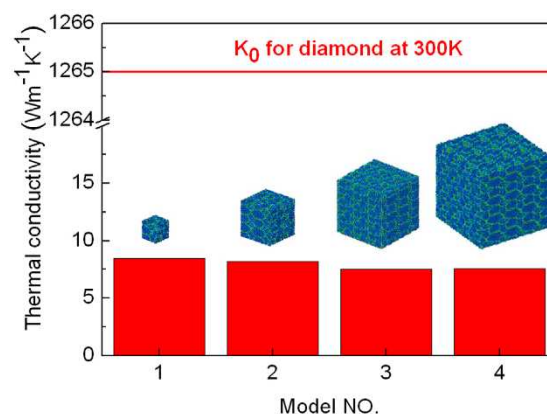

Figure 5 | Variation of thermal conductivity for nanocrystalline diamond with different simulation model sizes. The temperature is 300 K, and the grain size is 2.43 nm. The simulation cells of Models 1, 2, 3 and 4 are 40Å × 40Å × 40Å, 80Å × 80Å × 80Å, 120Å × 120Å × 120Å, and 160Å × 160Å × 160Å, respectively. They contain 8, 64, 216 and 512 grains, respectively.

grain size, single crystal thermal conductivity, single crystal PMFP, and the Kaptiza thermal resistance. The effectiveness of this model has been verified by comparing simulated value of ETC for nano-crystalline diamond at 300 K as well as experimental ETC for nano-crystalline silicon at 300 K with theoretical results based on this model. The relative importance of GBs and size effects of thermal properties on ETC of nanocrystalline diamond at 300 K has been studied by using this equation. With increasing grain size, both the effect of GBs and size effects of thermal properties become weaker, and the size effects become stronger than the GBs effect on thermal conductivity. This novel theoretical model provides a convenient path to the calculation of nanocrystalline materials thermal conductivity. It is expected that it will greatly contribute to in-depth understanding of the thermal properties of nanocrystalline materials.

Methods

In this work, the nanocrystalline diamond ETC are calculated by using the non-equilibrium molecular dynamics (NEMD) simulations[28,29]. This methodology uses an idea of imposing heat flux through the structure under study and determining a temperature gradient that develops as a consequence of the imposed flux[16]. The heat flux is introduced by continuously transferring energy from 'cold' regions, located at the ends of the simulation cell, to 'hot' regions, located at the middle of simulation model, as shown in Fig. 3 (a). Then, the ETC can be calculated from the heat flux and temperature gradient shown in Fig. 3 (b) by using the Fourier's law[26] (refer to supplementary discussion 1 about the detail of the computational method used here).

In order to carry out the simulation by using NEMD, the atomic models of nanocrystalline diamond are generated using the three-dimensional Voronoi tessellation method[30], which has been widely used in creating random grain structures for nanocrystalline materials simulation[31–33]. Fig. 4 shows a typical nanocrystalline diamond structure with periodic boundary conditions in all three-directions. All simulations have been performed using the large-scale atomic/molecular massively parallel simulation (LAMMPS) molecular dynamics package[34]. In these simulations, C-C bonding interactions have been described by Tersoff potential and an NPT ensemble has been used. We use the atmospheric pressure and temperature 300 K. The atomic coordinates and the overall periodic dimensions of the simulation cell were first optimized using the gradient-based minimization method implemented to minimize the stress. NEMD simulations have then been carried out on the relaxed structure to make the system equilibrated at room temperature with a time step of 0.1 fs for 2×10^5 steps. Then, by imposing a heat flux, the canonical ensemble has been performed consecutively for 10^6 steps to allow the systems reaching the steady-state regime. Finally, the temperature profiles have been obtained by averaging every 10^5 MD steps. In our simulations, the effects of domain size on ETC have been considered[17]. Four models with different domain sizes and the same grain size (2.43 nm) are listed in Fig. 5, as well as the separate ETCs calculated. It can be seen that the variation between the results obtained with these models is very small, although the simulation domain sizes are quite different.

1. Ni, B., Watanabe, T. & Phillpot, S. R. Thermal transport in polyethylene and at polyethylene–diamond interfaces investigated using molecular dynamics

simulation. *J. Phys.: Condens. Mat.* **21**, 084219; doi:10.1088/0953-8984/21/8/084219 (2009).
2. Yang, H.-S., Bai, G.-R., Thompson, L. & Eastman, J. Interfacial thermal resistance in nanocrystalline yttria-stabilized zirconia. *Acta Mater.* **50**, 2309–2317; doi: 10.1016/S1359-6454(02)00057-5 (2002).
3. Millett, P. C., Wolf, D., Desai, T., Rokkam, S. & El-Azab, A. Phase-field simulation of thermal conductivity in porous polycrystalline microstructures. *J. Appl. Phys.* **104**, 033512; doi: 10.1063/1.2964116 (2008).
4. Meyers, M. A., Mishra, A. & Benson, D. J. Mechanical properties of nanocrystalline materials. *Prog. Mater. Sci.* **51**, 427–556; doi: 10.1016/j.pmatsci.2005.08.003 (2006).
5. Nan, C.-W. & Birringer, R. Determining the Kapitza resistance and the thermal conductivity of polycrystals: A simple model. *Phys. Rev. B* **57**, 8264; doi: 10.1103/PhysRevB.57.8264 (1998).
6. Wang, S. *Thermal Conductivity of Nanocrystalline Nickel*, University of Toronto, (2011).
7. Cahill, D. G. *et al*. Nanoscale thermal transport. *J. Appl. Phys.* **93**, 793–818; doi: 10.1063/1.1524305 (2002).
8. Yang, H.-S., Eastman, J., Thompson, L. & Bai, G. *Grain-Size-Dependent Thermal Transport Properties in Nanocrystalline Yttria-Stabilized Zirconia*. (Cambridge Univ Press, 2001).
9. Angadi, M. A. *et al*. Thermal transport and grain boundary conductance in ultrananocrystalline diamond thin films. *J. Appl. Phys.* **99**, 114301; doi: 10.1063/1.2199974 (2006).
10. Shukla, P., Watanabe, T., Nino, J., Tulenko, J. & Phillpot, S. Thermal transport properties of MgO and $Nd_2Zr_2O_7$ pyrochlore by molecular dynamics simulation. *J. Nucl. Mater.* **380**, 1–7; doi: 10.1016/j.jnucmat. 2008.06.043 (2008).
11. Lawson, J. W., Daw, M. S., Squire, T. H. & Bauschlicher, C. W. Computational Modeling of Grain Boundaries in ZrB2: Implications for Lattice Thermal Conductivity. *J. Am. Ceram. Soc.* **95**, 3971–3978; doi: 10. 1111/jace.12037 (2012).
12. Crocombette, J.-P. & Gelebart, L. Multiscale modeling of the thermal conductivity of polycrystalline silicon carbide. *J. Appl. Phys.* **106**, 083520–083527; doi: 10.1063/1.3240344 (2009).
13. Aubry, S., Kimmer, C. J., Skye, A. & Schelling, P. K. Comparison of theoretical and simulation-based predictions of grain-boundary Kapitza conductance in silicon. *Phys. Rev. B* **78**, 064112; doi: 10.1103/Phys Rev B.78.064112 (2008).
14. Wang, Z., Alaniz, J. E., Jang, W., Garay, J. E. & Dames, C. Thermal conductivity of nanocrystalline silicon: Importance of grain size and frequency-dependent mean free paths. *Nano Lett.* **11**, 2206–2213; doi: 10. 1021/nl1045395 (2011).
15. Maldovan, M. Thermal energy transport model for macro-to-nanograin polycrystalline semiconductors. *J. Appl. Phys.* **110**, 114310–114317; doi: 10.1063/1.3665211 (2011).
16. Bagri, A., Kim, S.-P., Ruoff, R. S. & Shenoy, V. B. Thermal transport across twin grain boundaries in polycrystalline graphene from nonequilibrium molecular dynamics simulations. *Nano Lett.* **11**, 3917–3921; doi: 10.1021/nl202118d (2011).
17. Ju, S. & Liang, X. Thermal conductivity of nanocrystalline silicon by direct molecular dynamics simulation. *J. Appl. Phys.* **112**, 064305–064307; doi: 10.1063/1.4752266 (2012).
18. Bux, S. K. *et al*. Nanostructured bulk silicon as an effective thermoelectric materials. *Adv. Funct. Mater.* **19**, 2445–2452; doi: 10.1002/adfm.200900250 (2009).
19. Wang, X. [Unique feature of thermal transport in nanoscale and nanostructure materials] *Experimental Micro/nanoscale Thermal Transport*. [1–2] (John Wiley & Sons, Inc., New York, 2012).
20. Watanabe, T., Ni, B., Phillpot, S. R., Schelling, P. K. & Keblinski, P. Thermal conductance across grain boundaries in diamond from molecular dynamics simulation. *J. Appl. Phys.* **102**, 063503–063507; doi: 10.1063/1.1524305 (2007).
21. Che, J., Çağın, T., Deng, W. & Goddard III, W. A. Thermal conductivity of diamond and related materials from molecular dynamics simulations. *J. Chem. Phys.* **113**, 6888–6900; doi: 10.1063/1.2779289 (2000).
22. Gurevich, V. L. [Heat transfer] *Transport in phonon systems*. (North-Holland Publ., Amsterdam, 1986).
23. Abdi, H. [The method of least squares] *Encyclopedia of Measurement and Statistics*. [Neil, J. (ed.)] [1–7] (Sage Publication Inc., Thousand Oaks, CA, USA; 2007).
24. Glassbrenner, C. & Slack, G. A. Thermal conductivity of silicon and germanium from 3 K to the melting point. *Phys. Rev.* **134**, A1058; doi: 10.1103/PhysRev.134.A1058 (1964).
25. Han, Y.-J. & Chae, H.-B. Theoretical analysis of the thermal conductivity of diamond in a two-step model. *Phys. Rev. B* **52**, 27; doi: 1103/PhysRevB.52.27 (1995).
26. Guo, J., Wen, B., Melnik, R., Yao, S. & Li, T. Geometry and temperature dependent thermal conductivity of diamond nanowires: A non-equilibrium molecular dynamics study. *Physica E* **43**, 155–160; doi: 10.1016/j.physe.2010.06.032. (2010).
27. Huberman, M. & Overhauser, A. Electronic Kapitza conductance at a diamond-Pb interface. *Phys. Rev. B* **50**, 2865; doi: 10.1103/PhysRevB.50.2865 (1994).
28. Müller-Plathe, F. A simple nonequilibrium molecular dynamics method for calculating the thermal conductivity. *J. Chem. Phys.* **106**, 6082; doi: 10.1063/1.473271 (1997).
29. Müller-Plathe, F. & Reith, D. Cause and effect reversed in non-equilibrium molecular dynamics: an easy route to transport coefficients. *Comput. Theor. Polym. Sci.* **9**, 203–209; doi: 10.1016/S1089-3156(99)00006-9 (1999).
30. Ju, S., Liang, X. & Xu, X. Out-of-plane thermal conductivity of polycrystalline silicon nanofilm by molecular dynamics simulation. *J. Appl. Phys.* **110**, 054318–054317; doi: 10.1063/1.3633232 (2011).
31. Schiøtz, J., Di Tolla, F. D. & Jacobsen, K. W. Softening of nanocrystalline metals at very small grain sizes. *Nature* **391**, 561–563; doi: 10.1038/35328 (1998).
32. Fritzen, F., Böhlke, T. & Schnack, E. Periodic three-dimensional mesh generation for crystalline aggregates based on Voronoi tessellations. *Comput. Mech.* **43**, 701–713; doi: 10.1007/s00466-008-0339-2 (2009).
33. Watson, D. F. Computing the n-dimensional Delaunay tessellation with application to Voronoi polytopes. *J. Comput. Phys.* **24**, 167–172; doi: 10.1093/comjnl/24.2.167 (1981).
34. Plimpton, S. Fast parallel algorithms for short-range molecular dynamics. *J. Comput. Phys.* **117**, 1–19; doi: 10.1006/jcph.1995.1039 (1995).

Acknowledgments

Author contributions

B.W. conceived the project, H.D. and B.W. performed molecular dynamics simulations and analyzed the data, H.D., B.W. and R.M. co-wrote the paper. All authors discussed the results and commented on the manuscript.

Additional information

Supplementary information accompanies this paper at http://www.nature.com/scientificreports

Competing financial interests: The authors declare no competing financial interests.

How to cite this article: Dong, H., Wen, B. & Melnik, R. Relative importance of grain boundaries and size effects in thermal conductivity of nanocrystalline materials. *Sci. Rep.* **4**, 7037; DOI:10.1038/srep07037 (2014).

5